International Journal of Environmental Sciences
ISSN: 2229-7359
Vol. 11 No. 7, 2025
https://www.theaspd.com/ijes.php

Transient Thermal Analysis Of Finned Cross -Flow Heat Exchangers By Simulation

Amir Soroureddin[1*], Niloufar Sarabchi[2]
[1] Department of Mechanical Engineering, Azarbaijan Shahid Madani University, Tabriz, Iran
[2] Engineering and R&D Department of Pumpiran Co., Tabriz, Iran.
* Correspond Author: Soroureddin.a@azaruniv.ac.ir

Abstract
Cross-flow finned heat exchangers are used in various oil and gas industries. Finned heat exchangers are used in cases where the volume and weight of the exchanger are required to be low and the efficiency of the exchanger is high. These types of exchangers have fins or attachments on the main surface that are used to increase the heat transfer surface. Since the heat transfer coefficient on the gas side is much smaller than that of the liquid, finned heat transfer surfaces on the gas side are used to increase the heat transfer surface. Fins are widely used in gas-gas or gas-liquid heat exchangers where the heat transfer coefficient on one or both sides is small and a compact heat exchanger is required. This paper describes the importance of thermal process control, analyzes its performance problems, and presents a mathematical model of heat transfer processes in a heat exchanger. Three-dimensional simulations with sub-millimeter accuracy were performed with adaptive meshing, which was verified with GCI, and the Navier-Stokes RANS equations were solved with the k-omega SST turbulence model. The simulated boundary conditions included air flow velocities ranging from 2 to 5 m/s and a constant heating rate of 1.5 kW/m2 to the tube walls. The results showed that the heat transfer at the tips of the fins was up to 30% higher than in the middle regions due to the formation of turbulent vortices, and the Nusselt number for such a phenomenon was calculated to be 62.5. Finally, considering that the weight and volume of these fins are of particular importance due to their application, the effect of the materials and geometry of the heat exchanger profile on heat transfer were investigated.
Keywords: *Cross-flow finned heat exchangers, oil and gas industries, Navier-Stokes, Nusselt, Transient Thermal Analysis, Geometry*

1. INTRODUCTION

The attempt to investigate the performance of heat exchangers from various aspects has a long history, with most of this research being conducted on exchangers with circular cross-section tubes [1]. Since a heat exchanger with circular tubes has low heat transfer and relatively high pressure drop, transient thermal analysis in circular heat exchangers using finned fins is of particular importance. Also, the effect of the material and geometry of the fin profile can be among the factors affecting the increase in heat transfer for various applications [2-5].

Heat exchangers are used in all industrial, commercial, and everyday life fields that deal with energy exchange in some way, and are made in very small and very large sizes. The smallest ones (less than 1 watt) are used for electronic applications, superconductors, and the largest ones (heat capacity greater than 1000 MW) are used in large power plants and in chemical processes, cold stores, oil and gas and air conditioning, the automotive industry, the energy industry, power plants, refineries, metal smelting and glass industries, food and pharmaceutical industries, papermaking, etc. The phenomenon of heat transfer is used in various industries for cooling or heating fluids or performing chemical and physical processes. Systems designed for these industries must have the highest efficiency and the lowest possible weight [6]. Therefore, the use of finned tubes to increase the efficiency of the heat exchanger and reduce its dimensions is of great importance [7, 8]. In addition, the use of heat exchangers in line with the treaties It is internationally recognized for environmental protection because its use leads to reduced fuel consumption, reduced oil change intervals, and reduced production of chemical pollutants.

Several studies have been conducted in this field. In [9] numerically and experimentally investigated the energy storage system with a spiral tube and using paraffin and compressed graphite as PCM. The reduction in energy storage time occurs with increasing Reynolds number and temperature difference of the fluid with PCM. However, it should be noted that their simultaneous increase leads to more than the effective amount of heat loss and Reynolds should not exceed 8700. In [10] studied the heat transfer in a three-pipe exchanger using internal and external fins for melting a PCM material using fluent software. They discussed parameters such as the number of fins, fin length, Stefan number, materials used, and the effect of shape on the completion of melting in PCM. The results of their calculations showed that the effect of the shape of the fin in the tube requires a shorter time to complete melting in PCM, and the melting time reaches 34.7% of the case without fins. In [11] numerically investigated the thermal performance of a shell and tube heat exchanger. The numerical study followed the effect of fin on the efficiency of the exchanger under the influence of two independent adjustable parameters, namely fin pitch and fin height, while the surface roughness is constant. Finally, a new design of fins, spiral fins, was presented. The results presented were that fins generally increase the efficiency of the heat exchanger; and that spiral fins increase the efficiency of the heat exchanger by 17% compared to simple tubes.
Regarding energy and exergy analysis, in [12] investigated the performance of fins in a three-pipe heat exchanger in which the middle tube of PCM and hot water fluid were passed through the inner and outer tubes. The results showed that the energy efficiency of the three-pipe heat exchanger with fins was 71.8%. In [13] conducted a charging cycle of a coil thermal energy storage system on ice experimentally. The results were based on the fact that with increasing mass flow rate, heat transfer rate and energy efficiency increase, and also with increasing inlet temperature of the heat transfer fluid, the exergy efficiency increases. In [14] numerically investigated the performance of a phase change material in a three-pipe heat exchanger. The results showed that increasing the inlet temperature with a turbulent flow regime in HTF can improve the thermal performance, although the exergy efficiency decreases with increasing mass flow rate.
According to a review of studies conducted in the field of heat exchangers, it is observed that the effect of profile design and its material can be influential in heat transfer. Therefore, in this article, an attempt has been made to evaluate the effect of these parameters by simulating heat exchanger fan blades with respect to the weight and stiffness of the profile.

2. METHOD

Thermal design involves simply determining the heat transfer coefficients of the fluids on both sides to obtain the heat transfer coefficient in the unobstructed state (U). By considering a reasonable value for the obstruction coefficient, the overall heat transfer coefficient (Ud) is obtained, according to which and using the equation, $q = U_d.A\Delta T$ the required surface will be determined.

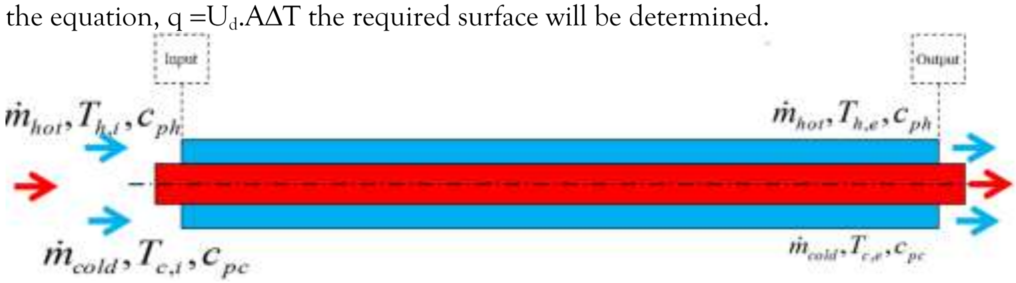

Figure 1: Heat exchanger schematic

For thermal design or predicting the performance of a heat exchanger, relationships between the overall heat transfer rate and quantities such as the fluid inlet and outlet temperatures, the overall heat transfer coefficient, and the heat transfer surface area must be obtained, which can be obtained by applying the overall energy balance for the two fluids, two relationships. For example, if q is the overall heat transfer rate between the hot and cold fluids, and the heat transfer between the heat exchanger and the environment and the changes in kinetic and potential energy are negligible, applying the energy balance, the result is [15]:

$q = m_h(h_{hi} - h_{ho})$	(1)
$q = m_c(h_{ci} - h_c)$	(2)

where h is the enthalpy of the fluid, the indices h, c refer to the cold and hot fluids, while i, o specify the inlet and outlet conditions. If no phase change occurs in any of the fluids and the specific heat is assumed to be constant, the above relations become as follows:

$q = m_h\, c_{p,h}(T_{hi} - T_{ho}) = m_c c_{p,c}(T_{ci} - T_{co})$	(3)

The temperatures appearing in these equations are the average temperatures at the relevant sections. The heat transfer equation can also be expressed as follows, where the average temperature difference along the exchanger replaces the temperature difference between the hot and cold fluids at a section: (ΔT_m is the average temperature difference along the exchanger)

$q = UA\Delta T_m$	(4)

The cooling system circuit in a magnetocaloric cooler consists of a plate regenerator acted upon by a magnet on a slide, a hot end heat exchanger (HHEX), a cold end heat exchanger (CHEX), their reservoirs, and a displacer. The circuit design necessitates multiple thermal processes including coolant flow, magnetocaloric effect of the regenerator, heat transfer between liquid and solid, heat transfer between the regenerator and the external environment, and heat transfer with the hot and cold reservoir. This requires a sophisticated mathematical apparatus for modelling the system that takes into account the variation of parameters over time. Controlling the state of the alternating magnetic field produced by the generator affects the magnetocaloric material (MCM) in the regenerator. The magnetocaloric effect depends on the material properties, the type of field and the presence of a regenerative circuit. The generator selects the required magnetic induction, depending on frequency for rotating models and displacement for traction models. In the regenerator, heat exchange takes place between the flowing coolant and the MCM, whose temperature changes according to the dependence on the magnetic field.

The regenerator consists of a plate part, heat exchangers with hot and cold ends and a displacer. The magnetic field is formed by changing the position of the magnet. Liquid and solid are considered incompressible and their properties are constant. The fluid flows along the x-axis, with velocity distribution along the y-axis. Pressure drop in the fluid is due to viscosity. A displacer in the form of two piston cylinders causes the working fluid to oscillate between the hot and cold ends. An electric heater maintains the temperature of the fluid required for the adiabatic change of the material. Sensors allow the parameters to be monitored during the cycle.The regenerator is made of magnetocaloric material, particularly gadolinium, which has a pronounced magnetocaloric effect. The regenerating fluid is demineralised water with ethylene glycol. The solid magnetic material and the fluid are modelled separately. The geometry of the regenerator has the shape of a parallelepiped.In modelling the heat exchange process, it must be taken into account that oil is a laminar flow and has variable rheological properties. Taking into account that the fluid is incompressible, viscous dissipation is neglected due to the small mass flow rate, so for modelling the form in the form of a system of differential equations can be written as follows [16]:

$$\begin{cases} \dfrac{\partial u}{\partial t} = -\dfrac{1}{\rho_j}\dfrac{\partial p}{\partial x} + v\left(\dfrac{\partial^2 u}{\partial x^2} + \dfrac{\partial^2 u}{\partial y^2} - \dfrac{\partial u}{\partial y}\right) + u\dfrac{\partial v}{\partial y} \\ \dfrac{\partial v}{\partial t} = -\dfrac{1}{\rho_j}\dfrac{\partial p}{\partial y} + v\left(\dfrac{\partial^2 v}{\partial x^2} + \dfrac{\partial^2 v}{\partial y^2} - \dfrac{\partial u}{\partial x}\right) - u\dfrac{\partial v}{\partial x} \\ \dfrac{\partial T_j}{\partial t} = \dfrac{k_j}{\rho_j C_j}\left(\dfrac{\partial^2 T_j}{\partial x^2} + \dfrac{\partial^2 T_j}{\partial y^2} + \dfrac{\partial^2 T_j}{\partial z^2}\right) - u\dfrac{\partial T_j}{\partial x} - v\dfrac{\partial T_j}{\partial y} \\ \dfrac{\partial T_{tv}}{\partial t} = \dfrac{k_{tv}}{\rho_{tv} C_{tv}}\left(\dfrac{\partial^2 T_{tv}}{\partial x^2} + \dfrac{\partial^2 T_{tv}}{\partial y^2} + \dfrac{\partial^2 T_{tv}}{\partial z^2}\right) \end{cases} \quad (5)$$

International Journal of Environmental Sciences
ISSN: 2229-7359
Vol. 11 No. 7, 2025
https://www.theaspd.com/ijes.php

where u, v are longitudinal and transverse velocities of the coolant flow, m/s; p pressure, Pa; ρ_j, ρ_{tv} are densities of liquid and solid, kg/m^3; C_j, C_{tv} are heat capacity, J/kg*K; k_j, k_tv are heat conductivity coefficients, W/m*K; T_j, T_{tv} are temperature at the point for liquid and solid, K; x, y, z are corresponding coordinates, m; t is time, s.

As initial conditions for the temperatures of the liquid and solid parts, the ambient temp of 293 is taken, for longitudinal and transverse velocities ±15 and 0, respectively. For the numerical solution of system, the finite difference method is applied: direct difference in time and right and left differences in spatial coordinates.

The boundary conditions for modeling this equations' system contain expressions characterizing the constant temperature at the inlet to the regenerator, the thermal insulation of the side surfaces, the equality of temperatures and heat flows at points at the interface of materials and the boundary conditions for the flow velocities.

$T_j(0,y,z,\tau)=T_{in},\ \tau>0,\ 0<y<L_y,\ L_{in}<z<L_y,$	(6)
$\frac{\partial T_j(L_x,y,z,\tau)}{\partial x}=0,\ \tau>0,\ 0<y<L_y,\ L_{in}<z<L_y,$	(7)
$\frac{\partial T_j(x,0,z,\tau)}{\partial y}=0,\ \tau>0,\ 0<x<L_x,\ L_{in}<z<L_y,$	(8)
$\frac{\partial T_j(x,L_y,z,\tau)}{\partial y}=0,\ \tau>0,\ 0<x<L_x,\ L_{in}<z<L_y,$	(9)
$\frac{\partial T_j(x,y,L_z,\tau)}{\partial z}=0,\ \tau>0,\ 0<x<L_x,\ 0<y<L_y,$	(10)
$\frac{\partial T_{tv}(0,y,z,\tau)}{\partial x}=0,\ \tau>0,\ 0<y<L_y,\ 0<z<L_{in},$	(11)
$\frac{\partial T_{tv}(L_x,y,z,\tau)}{\partial x}=0,\ \tau>0,\ 0<y<L_y,\ 0<z<L_{in},$	(12)
$\frac{\partial T_{tv}(x,0,z,\tau)}{\partial y}=0,\ \tau>0,\ 0<x<L_x,\ 0<z<L_{in},$	(13)
$\frac{\partial T_{tv}(x,L_y,z,\tau)}{\partial y}=0,\ \tau>0,\ 0<x<L_x,\ 0<z<L_{in},$	(14)
$\frac{\partial T_{tv}(x,y,0,\tau)}{\partial z}=0,\ \tau>0,\ 0<x<L_x,\ 0<y<L_y,$	(15)
$k_{tv}\frac{\partial T_{tv}(x,y,L_{in},\tau)}{\partial z}=k_j\frac{\partial T_j(x,y,L_{in},\tau)}{\partial z},$ $\tau>0,\ 0<x<L_x,\ 0<y<L_y,$	(16)
$T_{tv}(x,y,L_{in},\tau)=T_j(x,y,L_{in},\tau),$ $\tau>0,\ 0<x<L_x,\ 0<y<L_y,$	(17)
$\frac{\partial u(x,0,\tau)}{\partial y}=0,\ \tau>0,\ 0<x<L_x,$	(18)
$\frac{\partial u(x,L_y,\tau)}{\partial y}=0,\ \tau>0,\ 0<x<L_x,$	(19)
$\frac{\partial u(L_x,y,\tau)}{\partial x}=0,\ \tau>0,\ 0<y<L_y,$	(20)
$u(0,y,\tau)=u(x,y,0),\ \tau>0,\ 0<y<L_y,$	(21)

International Journal of Environmental Sciences
ISSN: 2229-7359
Vol. 11 No. 7, 2025
https://www.theaspd.com/ijes.php

$\frac{\partial v(0,y,\tau)}{\partial x}=0,\ \tau>0,\ 0<y<L_y,$	(22)
$\frac{\partial v(L_x,y,\tau)}{\partial x}=0,\ \tau>0,\ 0<y<L_y,$	(23)
$v(x,0,\tau)=v(x,L_y,\tau)=v(x,y,0),\ \tau>0,\ 0<x<L_x,$	(24)

The software implementation of the model was carried out in the ANSYS software. Each of the temperatures and flow rates arrays had 4 dimensions, including time and 3 spatial coordinates. The time step was set to 0.05 s.

3. RESULTS

Transient Thermal Response during Startup is presented in table 1. It shows the convective resistance, outlet temp & heat transfer rate as follows:

Table 1: Transient Thermal Behavior during Startup

Time (min)	Convective Resistance ($\times 10^{-3}$ K/W)	Outlet Temp. (K)	Heat Transfer Rate (W)
0	4.8	300.0	0
5	4.1	307.2	1,240
10	3.9	312.8	1,890
15	3.7	315.6	2,150

Transient thermal behavior has been shown in figure 2. The decrease in displacement resistance with time is related to the stabilization of the airflow and the formation of the boundary layer. This cyclic behavior and its applications in thermal management systems are very important.

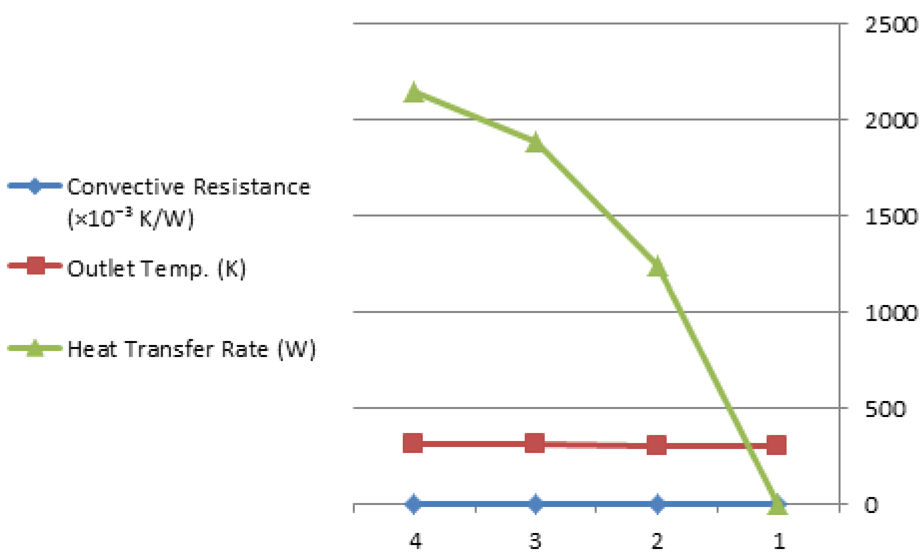

Figure 2: Transient Thermal Behavior

The residual plot for the velocity and continuity variables is shown in Figure 3-a. As the results show, the residual values for the variables converge after 115,000 iterations. Considering this plot and the accuracy and reliability of the results, the velocity contour over the fins is shown in Figure 3-b. As is clear, in the fluid inlet parts inside the fins, the velocity and consequently the heat transfer are high and with distance from the fluid inlet source, this heat transfer and velocity decrease.

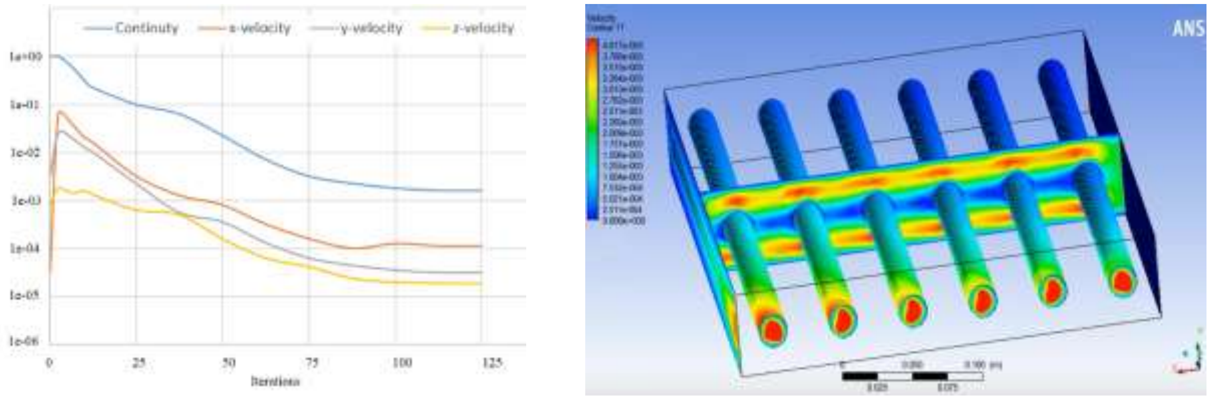

a. Residual for variables b. Fluid velocity contour in fins

Figure 3. Simulation results

For detail analysis the thermal and velocity conjures in 2-d conditions has been illustrated in figure 4. It shows the thermal counters (figure 4a) and flow velocity (figure 4b) in the tubes in this heat exchanger. As is clear, the yellow part of the tubes, where the hot water enters the tubes, has the highest possible velocity in the tubes. After the cold water enters the shell, the tubes begin to cool until they reach the U-shaped tube section, then the temperature increases due to the stillness and lack of fluid velocity in that section. The tubes begin to cool again in the return section.

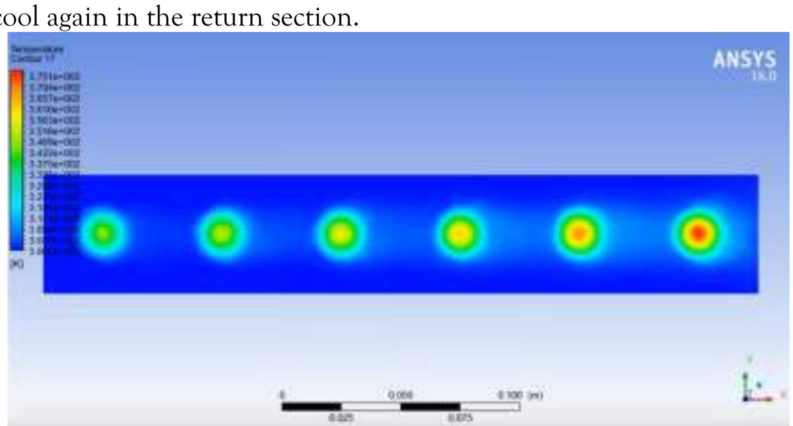

a) Temperature

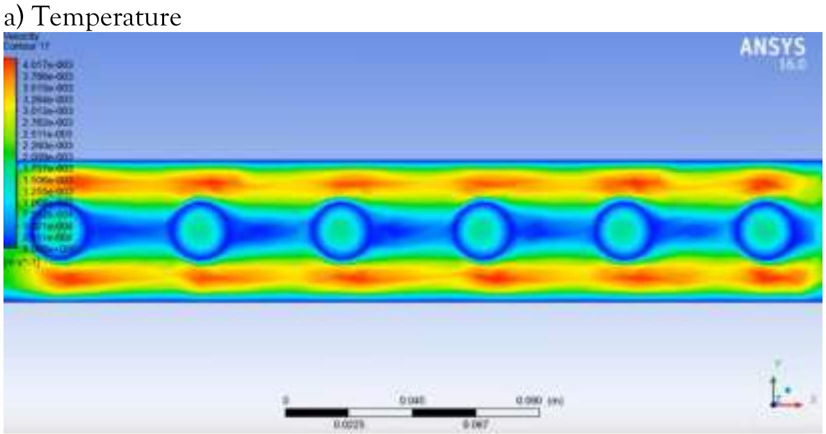

b) velocity

Figure 4. Thermal and velocity contour of fins

International Journal of Environmental Sciences
ISSN: 2229-7359
Vol. 11 No. 7, 2025
https://www.theaspd.com/ijes.php

For comparing the effect of the thermal rate with and without fin, the heat transfer rate has been compared in these two conditions. As shown in figure 5, since the air exchange contact surface has increased in cross fin mode, so heat transfer rate has been increased up to 42% in comparison to the without fin model.

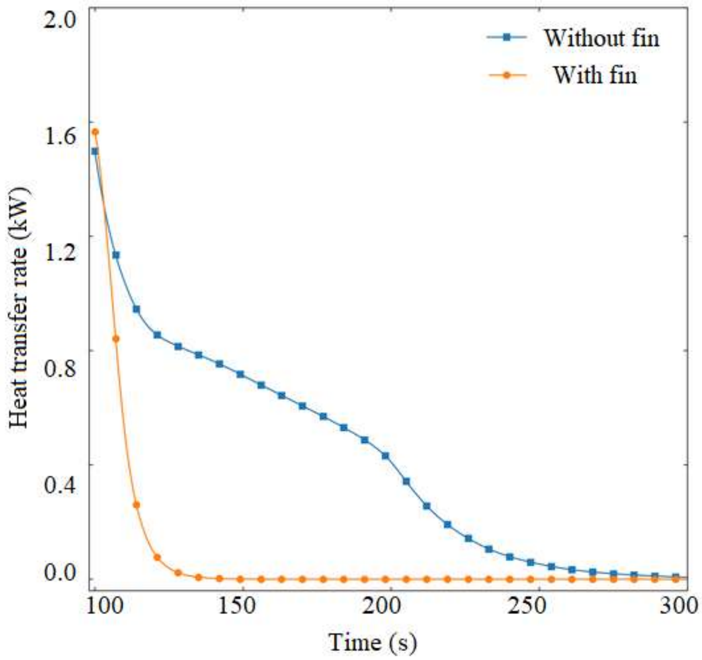

Figure 5. Heat transfer rate with and without fins

As shown in the figure, at the beginning of the shell, the temperature is the highest because the water exiting the upper floors pipes is collected in that part and, while creating vortex states, exchanges heat with the hot water inlet and outlet separator plate, which causes the temperature at that point to increase. Then, at the outlet, the lowest possible temperature is created due to the mixing of the average hot water from the back with the water exiting the lower floors pipes. After this temperature decrease, the temperature of that part increases due to the selection of the graph display points in the middle of the shell (between the upper and lower floors of the pipe).

3.1 Fin Materials and Comparative Performance

In this study, aluminum fins were compared with similar ones made of carbon. While copper reduced resistance by about 40%, its higher density (68%) made it unsuitable for applications where the weight of a component is a consideration. Carbon steel is more affordable, however regarding its lower thermal conductivity, it raises the thermal resistance up to 25%.

Table 2: Material Performance Comparison

Material	Thermal Conductivity (W/m·K)	Density (kg/m³)	Total Resistance (×10⁻³ K/W)
Al	236	2,7010	7.2
C-S	53	7,840	8.6
Co	402	8,970	4.3

4. CONCLUSION

In this paper, a finned heat exchanger has been simulated, which has been selected and designed to be the smallest possible in terms of dimensions and weight to include higher efficiency and lower manufacturing cost. The most important difference that can be mentioned as an innovation in this research is the effect of changing the geometry of the tube and the mass flow rate of fuel and oil on the heat transfer coefficient, Colburn coefficient, friction coefficient and outlet temperature changes, and also obtaining the best arrangement for the tubes and their weight and dimensions. This heat exchanger is used for heat transfer between fluids in the oil and gas industries. In order to investigate the effect of tube geometry on heat transfer rate, simulations were performed for a heat exchanger with finless tubes and again for the finned case, which indicates an increase in heat transfer of up to 30%. Also, the effects of changing the fluid mass flow rate and the profile material on the pressure drop of the exchanger and its heat transfer rate were investigated in order to achieve an optimal heat transfer model, while increasing work and energy efficiency, and reducing its environmental impacts.

REFERENCES

1. Singhal, M., Singh, S., Singla, R. K., Goyal, K., & Jain, D. (2020). Experimental and computational inverse thermal analysis of transient, non-linear heat flux in circular pin fin with temperature-dependent thermal properties. *Applied Thermal Engineering*, *168*, 114721.
2. Shariati, A., Azaribeni, A., Hajighahramanzadeh, P., & Loghmani, Z. (2013). Liquid–liquid equilibria of systems containingsunflower oil, ethanol and water. *APCBEE procedia*, *5*, 486-490.
3. Suárez, F., Keegan, S. D., Mariani, N. J., & Barreto, G. F. (2019). A novel one-dimensional model to predict fin efficiency of continuous fin-tube heat exchangers. *Applied Thermal Engineering*, *149*, 1192-1202.
4. Dube, A., Jaybhaye, M. D., More, P., & Jaybhaye, S. M. (2024). Study of variation in physiochemical properties of a worm gearbox lubricant by blending castor oil in the base lubricant. *Journal of Materials and Engineering*, *2*(4), 273-278.
5. Shaimi, M., Khatyr, R., & Naciri, J. K. (2022). Ansys mechanical automation using Python for the steady state thermal analysis of fins. In *Proceedings of the World Congress on Mechanical, Chemical, and Material Engineering, Prague, Czech Republic* (Vol. 8, pp. HTFF-178). Avestia.
6. Kumar, A., Kothari, R., Saxena, V., Sahu, S. K., & Kundalwal, S. I. (2022). Experimental investigation on paraffin wax-based heat sinks with cross plate fin arrangement for cooling of electronic components. *Journal of Thermal Analysis and Calorimetry*, *147*(17), 9487-9504.
7. Nikolic, A., Blagojevic, M., Zivkovic, M., Aleksic, A., & Savic, S. (2012). Software technologies for the analysis of blood flow in the human body. *International Journal of Industrial Engineering and Management*, *3*(2), 99-104.
8. Hailekiros, M. H., & YongPan, C. (2025). Numerical investigation of hydrogen absorption in solid hydride storage with novel tree-shaped fins. *International Journal of Hydrogen Energy*, *166*, 150893.
9. Chen, C., Zhang, H., Gao, X., Xu, T., Fang, Y., & Zhang, Z. (2016). Numerical and experimental investigation on latent thermal energy storage system with spiral coil tube and paraffin/expanded graphite composite PCM. *Energy conversion and management*, *126*, 889-897.
10 Sayehvand, H. O., Abolfathi, S., & Keshavarzian, B. (2023). Investigating heat transfer enhancement for PCM melting in a novel multi-tube heat exchanger with external fins. *Journal of Energy Storage*, *72*, 108702.
11. Amini, R., Amini, M., Jafarinia, A., & Kashfi, M. (2018). Numerical investigation on effects of using segmented and helical tube fins on thermal performance and efficiency of a shell and tube heat exchanger. *Applied Thermal Engineering*, *138*, 750-760.
12. Moghadam, F. N., Izadpanah, E., Shekari, Y., & Amini, Y. (2024). Experimental evaluation of shell geometry impact on thermal and exergy performance in helical coiled tube heat exchanger with phase change material. *Journal of Energy Storage*, *83*, 110790.
13. Abdelrahman, H. E., Refaey, H. A., Alotaibi, A., Abdel-Aziz, A. A., & Abd Rabbo, M. F. (2020). Experimental investigations on the thermal performance of an ice storage system using twin concentric helical coil. *Applied Thermal Engineering*, *179*, 115737.
14. Zhao, Y., & Mao, Q. (2024). Experimental and numerical analysis of unsteady state conditions on thermal storage performance of a conical spiral shell-tube energy storage system. *Journal of Energy Storage*, *88*, 111579.
15. Chen, Q., Hao, J. H., & Zhao, T. (2017). An alternative energy flow model for analysis and optimization of heat transfer systems. *International Journal of Heat and Mass Transfer*, *108*, 712-720.
16. Raju, K. S. (2011). *Fluid mechanics, heat transfer, and mass transfer: chemical engineering practice*. John Wiley & Sons.